SUPPLEMENTAL DATA

ASCE *Journal of Sustainable Water in the Built Environment*

Green Infrastructure Implementation in Urban Parks for Stormwater Management

Andrew Feldman, Romano Foti, and Franco Montalto

DOI: 10.1061/JSWBAY.0000880

© ASCE 2019

www.ascelibrary.org

Supplemental Materials

Thel-Mar Weir Flow Rate Calculation

Thel-Mar, LLC provided experimental flow rate data for the weir used in the analysis which is graphed in Fig. S1 (Thel-Mar 2015). The curve was divided into three sections (not shown) to provide the most accurate curve fit to translate water level above the Thel-Mar weir to volumetric flow rate as depicted as Case A in Fig. 3. The Akaike Information Criterion (AIC) statistical method determined the number of parameters for the curve fit. Hydraulic equations validated experimentally determined flow rates through the Thel-Mar weir. Fig. 3 also shows Case B flow situation of the addition of orifice flow through the rectangular and triangular sections of the weir and open channel flow above the weir.

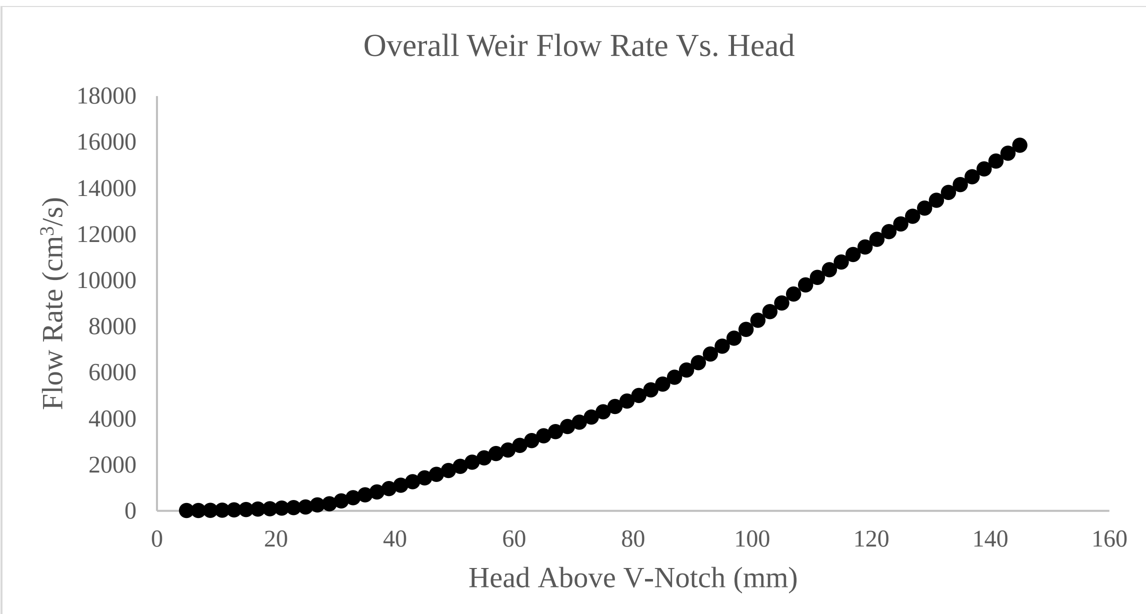

Fig. S1. Thel-Mar, LLC Experimental Weir Flow Data

Monitoring Project Logistics

In January 2012, an agreement was signed between Drexel University and the National Fish and Wildlife Foundation (NFWF) to retrofit a rain garden into Shoelace Park (Bronx, NY). The project team lead by the university included an engineering consulting firm (eDesign

Dynamics LLC) responsible for site assessment and design development, a landscape contractor (Olson's Creative Landscaping) responsible for construction, and a local quasi-governmental entity (Bronx River Alliance) to assist in maintenance activities. Drexel University was responsible for installation and maintenance of the monitoring equipment for a period lasting from October 2014 to June 2015. The total cost of the GI system over the project duration was $318,371 including costs of construction ($237,728), maintenance ($22,000), and monitoring ($58,643).

Pressure Transducer Calibration

In order to validate PT-A and PT-B readings, each sensor was placed in a container filled with water at 1.5 cm intervals. At each 1.5 cm interval, the manually measured water depth was compared to the pressure transducer reading (Table S1). In both cases, the pressure transducer readings correlated to the manual measurements with the coefficient of determination at nearly unity. The regression line equation generated from the calibration exercise was used to convert the raw pressure transducer reading to a calibrated reading for use in the analysis.

Calibrated PT-A and PT-B readings were successfully validated with in-situ measurements. The PT-A water level readings in the manhole at the conclusion of various storms did not align with the D_I measured invert throughout the monitoring period. However, in-situ manual measurements of water level in the manhole during various site visits between January 2015 and June 2015 compared closely with calibrated PT-A readings with a small root mean square error (RMSE) of 1.9 cm (Table S2). Similarly, the RMSE between the manual and calibrated PT-B readings was 1.2 cm (Table S3). In-situ measurements were performed only sporadically during the monitoring period and were thus solely used as a validation of the bucket calibration.

Table S1. PT-A and PT-B Bucket Calibration

1/21 Calibration	PT-A Measurements		PT-B Measurements	
Water Depth Measurement Number	Bucket Water Depth Measurement (cm)	Pressure Transducer Reading (cm)	Bucket Water Depth Measurement (cm)	Pressure Transducer Reading (cm)
1	1.52	1.22	1.68	0.15
2	2.74	3.05	3.05	1.62
3	4.27	4.72	4.42	2.74
4	6.10	6.25	6.10	4.51
5	8.08	8.53	7.32	5.79
6	9.72	9.54	9.39	7.92
7	10.67	10.73	10.97	9.42
8	11.95	12.07	12.25	10.94

Table S2. PT-A In-Situ Measurement Validation

PT-A In-Situ Measurements				
Date/Time	Manual Measurement (cm)	Raw PT-A Reading (cm)	Calibrated PT-A Reading (cm)	RMSE
1/19/2015 12pm	27.1	29.8	29.5	5.67
3/6/2015 1pm	35.1	35.6	35.3	0.06
3/12/2015 1:05pm	33.0	33.1	32.9	0.02
4/9/2015 2:00pm	33.0	34.1	33.8	0.60
4/17/2015 3:00pm	30.5	31.9	31.7	1.47
4/20/2015 11:50am	38.4	39.5	39.2	0.72
4/20/2015 11:55am	36.6	39.0	38.7	4.51
4/20/2015 12:00pm	36.3	39.4	39.1	8.17
4/20/2015 12:35pm	36.0	38.2	37.9	3.66
4/20/2015 12:40pm	35.7	38.5	38.2	6.70
4/20/2015 12:45pm	36.0	38.4	38.2	4.78
4/23/2015 2:05pm	29.2	29.9	29.6	0.18
5/11/2015 2:45pm	30.5	31.4	31.2	0.49
5/18/2015 2:25pm	20.3	24.5	24.3	15.78
5/26/2015 1:45pm	22.9	23.7	23.5	0.38
6/9/2015 10:40am	24.1	27.2	27.0	8.19
6/19/2015 2:25pm	22.9	23.0	22.8	0.01
			RMSE	1.90

Table S3. PT-B In-Situ Measurement Validation

PT-B In-Situ Measurements				
Date/Time	Manual Measurement (cm)	Raw PT-B Reading (cm)	Calibrated PT-B Reading (cm)	Percent Difference (%)
3/6/2015 1:10pm	4.9	3.2	4.7	0.03
4/9/2015 2:00pm	7.6	4.1	5.6	4.18
4/17/2015 2:45pm	5.1	5.1	6.6	2.32
4/23/2015 2:05pm	10.2	11.4	12.9	7.35
5/5/2015 2:30pm	5.1	3.6	5.1	0.00
5/11/2015 2:45pm	5.1	3.7	5.3	0.04
5/18/2015 2:45pm	7.6	6.3	7.8	0.02
5/26/2015 2:00pm	5.1	3.1	4.6	0.19
6/9/2015 10:20am	11.4	9.9	11.4	0.00
6/19/2015 2:10pm	5.1	4.2	5.8	0.46
			RMSE	1.21

Weir Invert Analysis

Once the water level in the manhole reaches the V-notch of the Thel-Mar weir located in the outlet pipe of the manhole, water begins to flow out of the manhole towards the rain garden. PT-A readings were used to estimate the water depth inside the manhole. Since the water level at the conclusion of various storms did not align with the D_I measured invert, the invert height was originally estimated as the calibrated PT-A reading corresponding to the end of flow through the Thel-Mar Weir. However, the average percent difference of 5.14% between in-situ measurements and PT-A readings validates the PT-A readings (Table S2) and the D_I constant invert was used to calculate flow through the Thel-Mar weir.

Performance Efficiency Evaluation

PE values deviated significantly from 100% in many cases (Table 4) and four possible explanations were evaluated:

(1) The C1 tributary area is larger than estimated where additional contributing areas other than the southern half of 228th Street and sidewalk exist. This includes areas such as Carpenter Avenue due to upstream combined sewer inlet blockages and unexpected water contributions from adjacent surfaces, such as nearby roofs or buildings. This scenario is likely as observations showed roof drains from adjacent structures contributing runoff to the stormwater inlet. However, while this may account for PE up to 300%, it does not, for example, explain an exceptionally high PE of 1100% recorded in the 07/07/15 storm. This also does not explain how this scenario would be more likely during a shorter storm with less accumulation (suggested by a significant, negative correlation between PE and both storm duration and depth).

(2) Turbulence from runoff entering the stormwater inlet basin causes erroneous PT-A readings. Anomalously high PT-A readings can result in overestimation of I_{228} and consequently *PE* as suggested by a laboratory experiment (discussed in "Catch Basin Crack Analysis" below). However, only one of the ten events with *PE* over 100% exhibited abnormally high PT-A reading spikes during rain events making this scenario unlikely.

(3) Obstructions in the stormwater inlet basin are present which hinder flow through the Thel-Mar weir. This would result in a flow through the Thel-Mar weir inconsistent with the hydraulic assumptions under which the flow equation is valid. While there is no direct observation supporting this scenario, obstructions were observed elsewhere in the system, such as in proximity of Combined Sewer Inlet B, resulting in invalidation of hydraulic assumptions.

(4) High intensity or longer storms may overwhelm the stormwater inlet leading to bypass and consequently lower *PE*. This is consistent with significant, negative correlations between *PE* and precipitation depths and storm durations. However, observations during the April 20, 2015 site visit during a substantial (88.9 mm) storm revealed that the design catchment

area was fully contributing to the stormwater inlet with little or no stormwater inlet bypass to Combined Sewer Inlet A. Nonetheless, storm durations were higher on average during the fall and winter months (Table 6) when no field observations during storms were made and *PE* was lowest supporting this scenario.

Ultimately, none of the scenarios have been fully refuted and thus it is possible that a larger C1 catchment area, turbulence from runoff entering the manhole, obstructions in the manhole, large storms overwhelming the stormwater inlet, or a combination of these scenarios contributed to anomalous *PE* observed throughout the monitoring campaign.

Rain Garden Obstructed Outflow

During a site visit on 4/20/15, Combined Sewer Inlet B was found to be clogged, causing surface ponding in the rain garden. In this case, *PR* would be underestimated where O_{RG} is overestimated via invalidation of Eq. 4 (constantly high *H*, but no actual flow). Evidence of similar occurrences with obvious inconsistencies between modeling assumptions and system behavior (with outflows greater than inflows yielding negative PR) was found during five precipitation events (December 8th, January 18th, March 14th, March 26th, and April 9th). These events had non-zero O_{RG} with rainfall depths of at least 31 mm. Thus, these storms were removed from the analysis (bringing total analyzed storms during the monitoring period from 31 to 26). It is possible the system exhibited this behavior during other events in which rain garden retention was underestimated.

Catch Basin Crack Analysis

In some instances throughout the monitoring period, PT-A readings suggested water depth continued to decrease below the level of the Thel-Mar weir during dry weather despite typically negligible loss phenomena (e.g. evaporation) in a closed manhole. Validation of PT-A readings in Table S2 suggests accurate PT-A readings throughout the monitoring period, though short term PT-A malfunction events are possible. Assuming a perfectly functioning PT-A, the possibility of a leak in the manhole was explored.

PT-A measurements suggest a crack in the concrete shell of the manhole approximately 9 cm below the Thel-Mar weir invert (25 cm above the manhole sump) during various storms throughout the monitoring period. The crack location was defined as the calibrated PT-A measurement where the water level became static after the duration of the storm. Here, an analysis is conducted to estimate the crack size with an idealized circular geometry exiting to open air outside of the manhole. The crack diameter was computed using a derivation of the orifice equation shown in Eq. S1. The coefficient of discharge was best estimated as a short tube equal to 0.8 (Street et al. 1996).

An average crack diameter of 0.34 cm was computed with results shown in Table S4. The water level above the crack was defined as the difference between the average PT-A reading in the manhole during the storm (located below the Thel-Mar weir) and crack location. The volumetric loss is the instantaneous volume change at the defined head above the crack and was calculated by multiplying the area of the manhole times the rate of change of the head. PT-A readings during March and April 2015 storms did not exhibit the same loss behavior and were not included in the analysis. A possible explanation for this is a dynamic groundwater table with saturated adjacent soil matrix causing inhibited flow during March and April 2015 and a dry adjacent soil matrix during all other storms throughout the monitoring campaign. A more comprehensive crack flow analysis will most likely compute a larger crack geometry, possibly non-circular, as the flowing water exits into the surrounding soil matrix more slowly than the idealized open-air situation. Nevertheless, dry weather outflows do not have an impact on the rain garden water balance. Additionally, the loss rate estimates through the crack (Table S4) are negligible in comparison to Thel-Mar weir inflow rates (Fig. S1) and will thus have a negligible impact on I_{228} estimates.

$$D = \sqrt{\frac{4 \times Q}{C \times \pi \times \sqrt{2gH}}} \qquad (S1)$$

D = Crack Diameter (cm)

H = Head Above Crack = Head – Crack Height (cm)

Q = Volumetric Loss at H (cm^3/s)

C = Coefficient of Discharge

g = 9.81 (m/s^2)

Table S4. Crack Analysis

Storm Date	Crack location head (cm)	Head Above Crack (cm)	Volumetric Flow Loss (cm^3/s)	Crack Area (cm^2)	Crack Diameter (cm)
10/29-10/30	23.59	1.01	4.51	0.13	0.40
10/31-11/2	22.93	1.48	1.5	0.03	0.21
11/6-11/7	24.73	4.39	3.04	0.04	0.23
11/12-11/14	22.68	0.91	4.51	0.13	0.41
11/17-11/18	22.56	0.97	1.5	0.04	0.23
11/24-11/25	23.32	1.43	1.5	0.04	0.21
11/26-11/29	24.17	0.94	1.5	0.04	0.24
12/1-12/2	24.96	0.64	6.01	0.21	0.52
12/2-12/4	25.17	0.31	3.01	0.15	0.44
12/5-12/7	25.14	0.37	3.01	0.14	0.42
12/8-12/12	25.02	2	6.01	0.12	0.39
12/16-12/18	25.75	2.18	3.01	0.06	0.27
12/22-12/25	32.54	0.7	6.01	0.20	0.51
12/27-12/28	32.7	1.24	4.51	0.11	0.38
1/3-1/5	32.67	0.09	7.52	0.71	0.95
1/12-1/14	27.02	4.31	1.5	0.02	0.16
1/18-1/19	29.15	3.49	1.5	0.02	0.17
4/19-4/24	28.9	1.91	1.5	0.03	0.20
5/16-5/20	24.14	2.21	1.5	0.03	0.19
6/5-6/7	24.07	2.22	3.01	0.06	0.27
6/7-6/10	24.56	2.16	1.5	0.03	0.19
6/14-6/16	23.44	2.82	7.52	0.13	0.40
6/16-6/17	23.26	3.22	7.52	0.12	0.39
6/27-6/29	23.11	1.3	3.01	0.07	0.31
6/30-7/3	23.23	1.76	1.5	0.03	0.20
7/7-7/8	23.41	4.22	10.52	0.14	0.43
7/8-7/9	23.62	3.55	7.52	0.11	0.38
7/9/2015	23.47	4.43	6.01	0.08	0.32
7/9-7/10	23.41	3.47	4.51	0.07	0.29

Investigation of Turbulent Manhole Inflows on PT-A

Due to the occurrence of large *PE* throughout the monitoring period, the possibility that erroneous PT-A readings occurred as a result of turbulence from runoff entering the manhole via the stormwater inlet on 228^{th} Street was investigated in a laboratory experiment. PT-A readings suggested significant abnormal instantaneous changes in head, or spikes, in water levels over five-minute intervals during various events. The goal was to determine the effect of turbulent inflow into the bucket on pressure transducer readings. Results indicate instantaneous pressure transducer reading changes from 16 cm to 48 cm from a turbulent stream of inflow entering the bucket. Five storms throughout the monitoring period exhibited large instantaneous changes in PT-A readings. When the effects of the spikes are removed, *PE* is reduced 48% on average. While this can account for some larger than average *PE*, this does not fully explain *PE* as high as 1100% recorded during the 07/07/15 Storm.

Rain Garden Retention Extrapolation

It was determined that a storm depth of approximately 10 mm produced the upper limit on the amount of runoff volume that the rain garden could retain. Based on simple linear regression in Fig. S2, a 10 mm storm results in approximately 8.6 m^3 of runoff retained without outflow. Conservatively, dividing this volume by a 25 mm storm depth suggests that the rain garden can retain a tributary area of 344 m^2 in this storm. This is on an area nine times the rain garden size or a hydraulic loading ratio of 9:1.

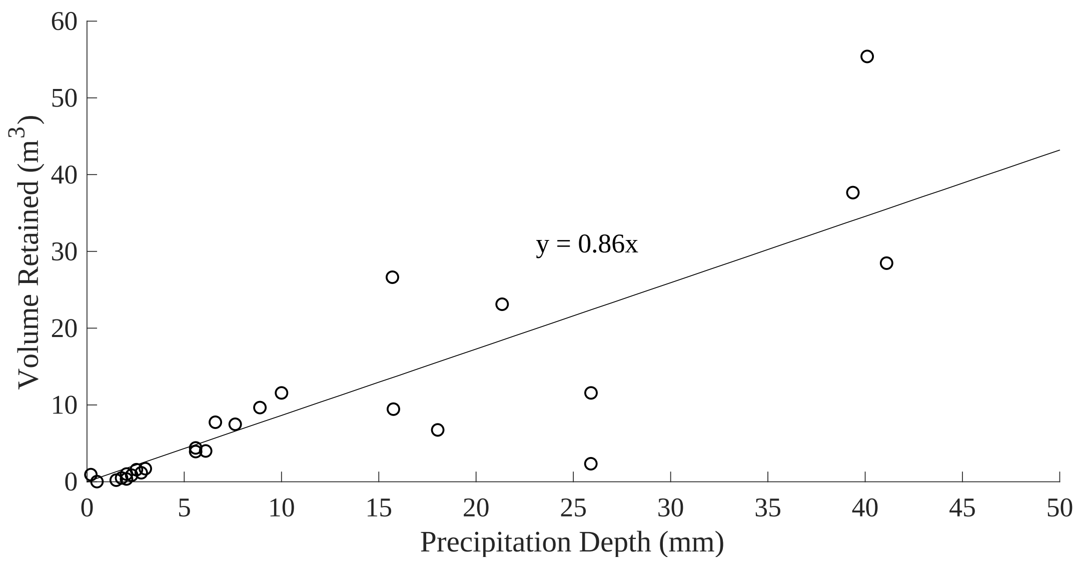

Fig. S2. Rain Garden Retention Regression. Note that the R^2 is 0.7.

References

Street, R., Watters, G., Vennard, J. (1996). *Elementary Fluid Mechanics*, 7th Ed., Wiley, Canada.

Thel-Mar (2015). “12 inch Thel-Mar Co. Volumetric Weir Discharge Table”. Thel-Mar Company.